Cobalt-related defects in silicon

T. M. Gibbons, D. J. Backlund, and S. K. Estreicher[a)]
Physics Department, Texas Tech University, Lubbock, Texas 79409-1051, USA

(Received 26 October 2016; accepted 17 January 2017; published online 27 January 2017)

Transition metals from the 3d series are unavoidable and unwanted contaminants in Si-based devices. Cobalt is one of the most poorly understood impurities with incomplete experimental information and few theoretical studies. In this contribution, the properties of interstitial cobalt (Co_i) in Si and its interactions with the vacancy, self-interstitial, hydrogen, and substitutional boron are calculated using the first-principles tools. The stable configurations, gap levels, and binding energies are predicted. The activation energy for diffusing Co_i is calculated with the nudged-elastic-band method and found to be slightly lower than that of interstitial copper and nickel. The binding energies and gap levels of the substitutional cobalt (Co_s) and of the {Co_s,H} and {Co_s,H,H} complexes are close to the experimental data. The properties of the cobalt-boron pair are calculated. *Published by AIP Publishing.*
[http://dx.doi.org/10.1063/1.4975034]

I. INTRODUCTION

Cobalt is a common transition-metal impurity in Si-based devices.[1] Its high-temperature solubility ($\sim 10^{15}$ cm^{-3} at 1100 °C) is slightly less than that of Ni and Cu. When introduced at high temperatures, Co almost entirely precipitates during cool-down[2] at internal voids[3] or other defects. Some precipitates can short p-n junctions.[2] It also forms silicides[4] in the cubic fluoride structure[1] with little disruption to the host crystal because $CoSi_2$ has a lattice constant within 1.2% of that of Si. In the solar-grade Si materials, the negative impact of a (total) Co concentration of the order of 10^{16} cm^{-3} is comparable to (slightly less than) that of Fe.[5] However, less than 0.1% of the total Co present in the sample is electrically active.[1,2,6,7] Because of its low solubility at room temperature and its very high diffusivity, the concentration of interstitial Co is too low to be detected by electron paramagnetic resonance (EPR),[8] even though neutron activation analysis shows that Co is present.[2,7]

The Mössbauer studies[7,9] show that the dissolved interstitial cobalt (Co_i) is predominantly at tetrahedral (T) sites and that as much as 10^{14} cm^{-3} substitutional cobalt (Co_s) is also present after in-diffusion at 940 °C. The Mössbauer channeling experiments[9] also show Co_i at off-center tetrahedral interstitial (T) sites, a spectrum attributed to the interstitial cobalt – substitutional boron pair {Co_i,B_s} as well as Co at unidentified multi-vacancy complexes.

The high-temperature diffusivity of interstitial cobalt (Co_i) is comparable to that of interstitial Cu or Ni.[10,11] The activation energy for the migration of 0.37 eV has been measured in the range of 760–1100 °C using the tracer method (with ^{57}Co).[12]

The deep-level transient spectroscopy (DLTS) has been used by numerous authors to study the electrical level of Co-related defects in Si,[13–24] but the proposed assignments of the DLTS peaks to specific Co-related defects have resulted in considerable confusion.[1,6,7,17,25–27] The same peaks have been assigned to acceptor or donor levels of Co_i, Co_s, the Co_iB_s pair, and a range of Co-H complexes. It took a substantial effort and a combination of experimental techniques to clarify the situation. Scheffler *et al.*[25–27] have used DLTS, Laplace-DLTS, and minority-carrier transient spectroscopy (MCTS), combined with annealing studies, electric-field dependence (Poole-Frenkel effect), depth profiling, and hydrogenation from wet-chemical etching as well as remote plasma exposure in p- and n-type FZ-Si samples doped with Co during growth. The results of these studies are as follows.[26]

No DLTS peak has been assigned to Co_i. All the other defects containing one Co atom have one acceptor (−/0), but no donor level. In the case of Co_s, the acceptor level is at $E_c-0.39$ eV (E200) and the DLTS peak anneals out at 600 °C. In the case of the Co_iB_s pair, it is at $E_v+0.46$ eV (H240) and anneals out below 150 °C. In the case of {Co_s,H}, it is at $E_c-0.35$ eV (E200′) and anneals out at 300 °C. Finally, in the case of {Co_s,H,H}, it is at $E_c-0.29$ eV (E140) and anneals out above 300 °C. The other peaks often reported in the DLTS spectra do not correlate with Co-related defects. For example, the E90 peak at $E_c-0.17$ eV is associated with the carbon-hydrogen pair, while the H160 peak at $E_v-0.38$ eV has not been identified but involves H and not Co.

Thus, very little atomic-level experimental information about isolated Co in Si is available. The details about the sites, spin states, binding and migration energies, and interactions with impurities and native defects are lacking.

The early theoretical studies involving Co in Si involved very small clusters and/or approximate electronic-structure methods. The focus was on trends rather than quantitative predictions. Hemstreet[28] considered Co_s in the Si_4CoH_{12} cluster using the scattering-Xα method, while DeLeo *et al.*[29] used the same method for Co_i in the $Si_{10}CoH_{16}$ cluster. The local-density Green's function method[30,31] (without total energies or geometry optimizations) was used to predict the gap levels of isolated Co in Si: Co_s is found to have an acceptor level just below the conduction-band minimum,

[a)]stefan.estreicher@ttu.edu

while Co_i has double- and single-acceptor levels at $E_v + 0.2$ eV and $E_v + 0.5$ eV, respectively.

Utzig[32] used an elastic energy approach to estimate the activation energy for diffusing interstitial cobalt, nickel, and copper and found 0.37 eV, 0.47 eV, and 0.43 eV, respectively.

Beeler *et al.*[33,34] used Green-functions based on the linear muffin-tin-orbital method in the atomic-sphere approximation. They found[34] that Co_i has a donor level at $E_v + 0.35$ eV and an acceptor level at $E_c - 0.16$ eV (Co_i^+, Co_i^0, and Co_i^- have been found to have spin states of 0, 1/2, and 0, respectively). They predicted[34] that Co_s has a donor level at $E_v + 0.62$ eV and single- and double-acceptor levels at $E_c - 0.39$ eV and $E_c - 0.29$ eV, respectively. The spin states of Co_s in the +, 0, −, and 2− charge states are 0, 1/2, 1, and 3/2, respectively.

Kamon *et al.*[35] performed the first-principles calculations (augmented plane waves, local-density approximation) and obtained the migration barriers for Co, Cu, and Ni to be 0.25, 0.31, and 0.35 eV, respectively. Matsukawa *et al.*[36] estimated these migration barriers from the total energy difference between the T and hexagonal interstitial sites in the Si_{64} supercell to be about 0.3, less than 0.1, and 0.1 eV, respectively.

Zhang *et al.*[37] performed the first-principles calculations for interstitial and substitutional V, Cr, Mn, Fe, Co, and Ni with the generalized gradient approximation in small supercells. Their aim was to discuss their magnetic behavior. They predicted that the formation energy of Co_s is 0.3 eV higher than that of Co_i. They did not discuss gap levels or migration barriers.

In this work, we present the results of first-principles calculations for Co_i, its interactions with the vacancy and the self-interstitial. The complexes involving Co_i or Co_s and one of two H interstitials are calculated. The activation energy for diffusing of Co_i^0 is obtained using the nudged-elastic-band (NEB) method. The gap levels of the stable defects are predicted using the marker method. The level of theory is discussed in Section II. Section III contains the results and the key points are summarized in Section IV.

II. METHODOLOGY

Our spin-density-functional calculations are based on the SIESTA method[38,39] in the Si_{216} periodic supercells. This combination of tools has been used for other 3d TM impurities: Ti,[40,41] V,[42] Fe,[43–45] Ni,[46] and Cu.[47–49] The lattice constant of the impurity-free cell is optimized in each charge state, and the defect geometries are obtained with a conjugate gradient algorithm. A $3 \times 3 \times 3$ Monkhorst-Pack[50] mesh is used to sample the Brillouin zone.

The electronic core regions are removed from the calculations using the Troullier–Martins norm-conserving pseudopotentials[51] developed for SIESTA.[52] All the pseudopotentials have relativistic and core corrections. The Co pseudopotential includes semicore 3s and 3p states.

The valence regions are treated with spin-density-functional theory within the revised generalized gradient approximation for the exchange-correlation potential.[53] This potential leads to the prediction of accurate activation energies for diffusion of impurities in Si.[54] The charge density is projected on a real-space grid with an equivalent cutoff of 350Ryd to calculate the exchange-correlation and Hartree potentials. The basis sets for the valence states are linear combinations of numerical atomic orbitals:[55,56] double-zeta for elements of the first two rows of the Periodic Table (H to Ne) to which a set of polarizations functions (five 3d's) are added for Si. The basis sets of Co include two sets of s and d orbitals and one set of p's.

The gap levels are evaluated using the marker method[57,58] with the perfect crystal as the universal marker for all the defects: the reference donor and acceptor levels are the top of the valence band and the bottom of the conduction band, respectively. This works well for a wide range of defects provided that the defect geometries and the lattice constant of the supercell are optimized in each charge state with a $3 \times 3 \times 3$ k-point sampling. This produces converged energies for the supercell size used here.

The migration paths and activation energies are calculated using the nudged elastic band (NEB) method[59] in the Si_{64} supercell with a $2 \times 2 \times 2$ Monkhorst–Pack mesh because of the substantial amount of computer required in the NEB calculations. Our implementation uses the climbing image method[60] for finding the saddle points. Local tangents are estimated using the improved-tangent formalism.[61] The springs connecting the images have a spring constant of 0.1 eV/Å. The converged diffusion path is the one for which the maximum force component perpendicular to the path at each image is less than 0.04 eV/Å. This cell size and k-point sampling have been shown to predict very accurate migration barriers for isolated impurities in Si.[54]

III. RESULTS

A. Co_i and its interactions with the vacancy and the Si self-interstitial

The T site is the only minimum of the potential energy for Co_i in Si. Interstitial configurations that involve substantial lattice relaxation such as the bond-centered site are much higher in energy and unstable. Co_i in Si is at a slightly relaxed T site in the neutral charge state with spin 3/2, which we denote $^{3/2}Co_i^0$. But $^{1/2}Co_i^0$ is only 0.06 eV higher in energy. Note that in free space, there is no difference in energy between the two spin states. The small value (0.06 eV) means that interstitial Co does not interact much with its surrounding. Indeed, the energy difference between spin states can be much larger in covalently bound configurations (see the interactions with the vacancy and the self-interstitial below) because the electrons pair up in covalent bonds. Changing the spin from 1/2 to 3/2 means promoting one electron from a bonding to an anti-bonding orbital. A Mulliken population analysis shows that 98% of the spin density is in the orbitals of the Co atom, with +4.7% distributed on its Si nearest neighbors and −2.8% on its second-nearest neighbors.

The calculated distance between Co_i and its four Si nearest neighbors is 2.424 Å, slightly larger than the T−Si distance in the impurity-free supercell, 2.383 Å. The marker method predicts the donor level to be just below the top of the valence band and the acceptor level to be far above the bottom of the conduction band. Thus, Co_i is always in the

neutral charge state in Si. No DLTS peak has been associated with Co_i,[26,27] but this could also be a consequence of its very fast diffusion.

Interstitial cobalt migrates along T-hexagonal-T sites with a saddle point at the hexagonal interstitial site. The calculated activation energy for diffusion is 0.15 eV. For comparison, the activation energies for diffusing Cu_i^+ and Ni_i^0 calculated at the same level of theory are 0.18 eV[54] (measured: 0.18 ± 0.01 eV[62]) and 0.21 eV[54] (measured: 0.15 ± 0.04 eV[46]), respectively. Thus, Co_i^0, Ni_i^0, and Cu_i^+ are among the fastest-diffusing impurities in Si.

The vacancy in Si (V_{Si}) is a negative-U defect stable in the 2+, 0, and 2− charge states with spin 0.[63] The double-donor level (+/++) is located at $E_v + 0.13$ eV, above the first donor level (0/+) at $\sim E_v + 0.05$ eV[64] (the location of the second acceptor level is not known). When $^{3/2}Co_i^0$ interacts with a *pre-existing* vacancy $^0V_{Si}^0$, it becomes $^{3/2}Co_s$ and then $^{1/2}Co_s$: $^0V_{Si}^0 + {}^{3/2}Co_i^0 \rightarrow {}^{3/2}Co_s^0 + 2.72$ eV followed by $^{3/2}Co_s^0 \rightarrow {}^{1/2}Co_s^0 + 0.45$ eV. Note that the theoretical two-step process occurs because the geometries are optimized with a fixed spin. In the real world, the spin flips as Co traps in the vacancy.

The net 3.17 eV energy gain is the binding energy of Co_i to the vacancy and should be compared to the formation enthalpy of the vacancy. This number is difficult to pin down precisely. The positron annihilation experiments[65] gave 3.6 ± 0.2 eV, a value lower than the one extracted from the self-diffusion experiments: 3.6–4.0 eV[66] and about 4.2 eV,[67] respectively. The value calculated at the present level of theory is 4.0 eV.[68]

Note that the vacancy is an orbital triplet and therefore Jahn-Teller is unstable in T_d symmetry in all but the 2+ charge state. Calculating the Jahn-Teller energy correction requires including electron-phonon coupling and therefore abandoning the Born-Oppenheimer approximation. The Jahn-Teller correction is not included here, and the total energy of the vacancy is slightly off.

Thus, isolated Co in Si should remain interstitial unless vacancies are provided by implantation, irradiation, surface treatments, high-T anneals, or other energetic processes. The binding energy of Co_i to the vacancy is slightly larger than that calculated for Ti[40] (∼2.0 eV), V[42] (∼3.0 eV), Fe[44] (∼2.9 eV), and Ni[40] (∼2.6 eV), and comparable to Cu[49] (∼3.1 eV). This corresponds to the bond strengths of about 0.5–0.9 eV for each of the four TM-Si bonds. The calculated TM-Si distances for $^{1/2}Co_s^0$ and $^1Co_s^-$ are 2.238 and 2.245 Å, respectively, as compared to the Si−Si distance of 2.383 Å in the impurity-free supercell. We find Co_s to have an acceptor level at $E_c - 0.44$ eV and no donor level.

Co_i is unlikely to interact directly with an isolated self-interstitial (I_{Si}) in Si. Indeed, I_{Si} quickly precipitates or expels substitutional impurities (such as C) and is likely to do that long before it encounters Co_i (its concentration is very low). However, the strained environment at a self-interstitial is to some extent comparable to that found near the dislocations or grain boundaries. The interactions between an interstitial TM impurity and a self-interstitial give us an estimate of the energetics of an interstitial TM interacting with the strained Si-Si bonds. The reaction

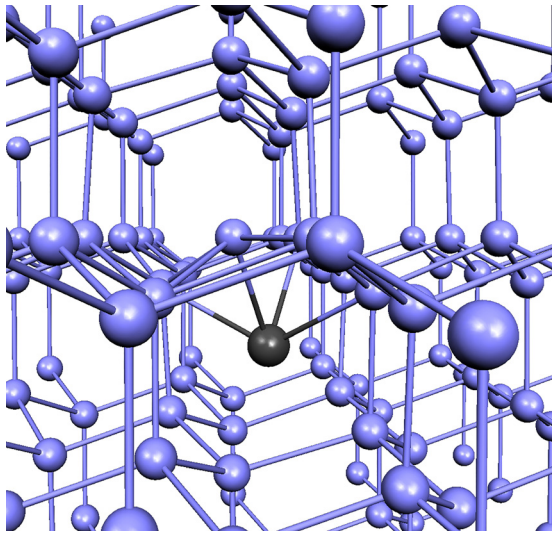

FIG. 1. The $^{1/2}\{I_{Si},Co_i\}^0$ defect. The Si atoms are blue (light grey) and Co is black.

is $^0I_{Si}^0 + {}^{3/2}Co_i^0 \rightarrow {}^{3/2}\{I_{Si},Co_i\}^0 + 0.59$ eV followed by $^{3/2}\{I_{Si},Co_i\}^0 \rightarrow {}^{1/2}\{I_{Si},Co_i\}^0 + 0.37$ eV, leading to a total gain in energy of 0.96 eV (Fig. 1). We find that the $\{I_{Si},Co_i\}$ defect has an acceptor level at $E_c - 0.17$ eV, with spin 0 in the negative charge state.

B. Cobalt-hydrogen interactions

Co_i reacts with bond-centered (bc) hydrogen $^0H_{bc}^+$ or $^{1/2}H_{bc}^0$, but the binding energies are small: $^{3/2}Co_i^0 + {}^{1/2}H_{bc}^0 \rightarrow {}^1\{Co_i,H\}^0 + 0.51$ eV and $^{3/2}Co_i^0 + {}^0H_{bc}^+ \rightarrow {}^{1/2}\{Co_i,H\}^+ + 0.37$ eV (the spin flip accounts for 0.09 eV). The other plausible configurations (with H bound to Si atoms near Co_i) are higher in energy. Such low binding energies resulting from the nearly full 3d orbitals of Co have been reported in the case of Ni_i as well.[41] The $\{Co_i,H\}$ pair has an acceptor level at $E_c - 0.18$ eV. The $\{Co_i,H\}$ pair is at best marginally stable at room temperature.

Co_s is much more likely to trap interstitial hydrogen: $^{3/2}Co_s^0 + {}^{1/2}H^0_{bc} \rightarrow {}^{3/2}\{Co_s,H\}^0 + 1.43$ eV (Fig. 2). This defect

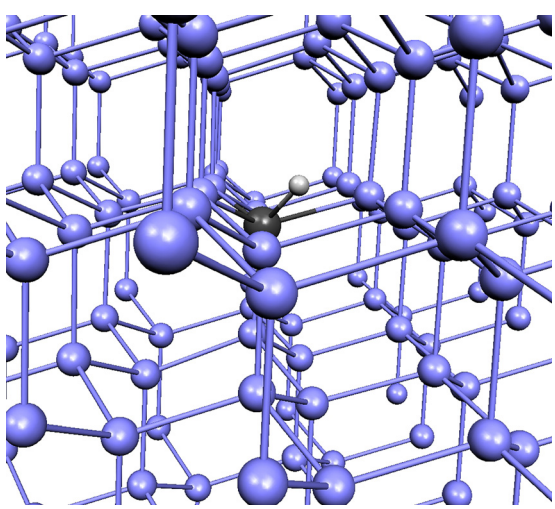

FIG. 2. The $^{3/2}\{Co_s,H\}^0$ defect: Si atoms are blue (light grey), H is the white small ball, and Co is black.

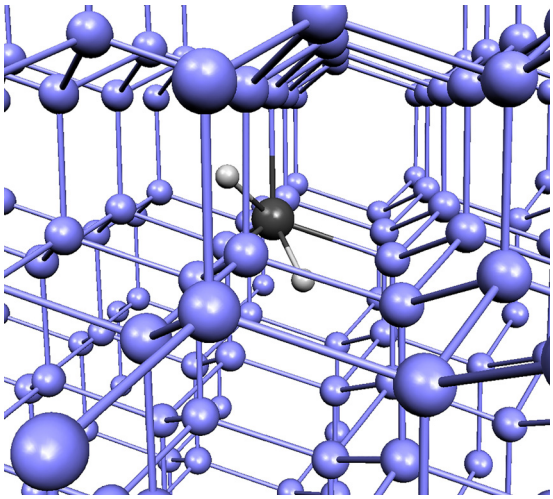

FIG. 3. The $^{1/2}\{Co_s,H,H\}^0$ defect: Si atoms are blue (light grey), the H's are the (white) small balls, and Co is black.

has an acceptor level at $E_c-0.27$ eV (measured: $E_c-0.35$ eV[26]). The interaction with a second H leads to the formation of $^{1/2}\{Co_s,H,H\}^0$ (Fig. 3) with an energy gain of 1.67 eV. This defect has an acceptor level at $E_c-0.42$ eV (measured: $E_c-0.29$ eV[26]). Note that H prefers attaching directly to the substitutional transition metal (which becomes 5- or 6-fold coordinated) rather than binding to the nearby Si atoms (which causes additional lattice relaxation).

C. Cobalt-boron interactions

Interstitial cobalt reacts with substitutional boron and forms a trigonal pair (Fig. 4): $^{3/2}Co_i^0 + {}^0B_s^- \rightarrow {}^{3/2}\{Co_i,B_s\}^- + 0.55$ eV (the trigonal configuration with Co_i at the antibonding site of an Si nearest to B_s is 0.12 eV higher in energy). This binding energy is somewhat lower than that of $\{Fe_i,B_s\}$ (0.65 eV[43]) calculated at the same level of theory. However, in the case of cobalt, the interactions do not involve a Coulomb term. The temperature at which such a pair is expected to dissociate is mostly dictated by the

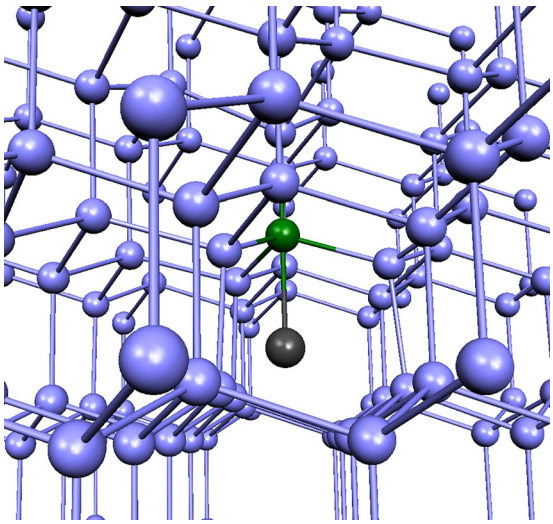

FIG. 4. The $^{3/2}\{Co_i,B_s\}^-$ defect. The Si atoms are blue (light grey), B is green (darker grey), and Co is black.

configurational entropy contribution to the free energy.[69] In the case of B-O complexes, it is about 0.5 eV at room temperature.

The $\{Co_i,B_s\}$ pair has an acceptor level at $E_c-0.36$ eV. This value does not agree well with the measured one, $E_c-0.71$ eV.[26] We examined all the usual culprits (B pseudopotential, exchange-correlation potential, different configurations, etc.), but the reasons for this discrepancy remain unclear.

IV. KEY POINTS

Interstitial cobalt in Si is the electrically inactive $^{3/2}Co_i^0$ impurity. It diffuses interstitially with the remarkably low activation energy of 0.15 eV, which is less than half the measured value of 0.37 eV.[12] In the case of Cu_i, the Hartree-Fock calculations predicted 0.24 eV,[70] which was about half the accepted value at the time, 0.43 eV.[71] Later experiments confirmed the low value[62] (0.18 ± 0.01 eV) and NEB calculations[40] produced 0.18 eV as well. It is likely that the measurements in the original B-doped samples[12] involved the trap-limited diffusion of Cu_i^+, which was slowed-down by its interactions with B_s^-. In the case of Ni_i, the accepted migration barrier of 0.47 eV[72] was also challenged by the NEB calculations, which predicted a much lower value 0.21 eV.[40,54] Later experiments[46] showed that the actual activation energy is 0.15 ± 0.04 eV, close to the NEB value. It will be interesting to see if history repeats itself in the case of Co_i since the Co diffusivity was also measured in B-doped Si.

If a vacancy is provided, $^{3/2}Co_i^0$ becomes $^{1/2}Co_s^0$ with an energy gain of 3.17 eV. Co_s has a single acceptor level at $E_c-0.44$ eV (measured:[26] $E_c-0.39$ eV). The DLTS line anneals out at 600 °C.

The interactions between Co_i and an Si self-interstitial lead to the formation of the $^{1/2}\{I_{Si},Co_i\}^0$ pair with an energy gain just below 1 eV. This pair has an acceptor level at $E_c-0.17$ eV.

The interactions between Co_i and hydrogen are weak. The pair has a binding energy of 0.37 eV and is therefore unlikely to survive at room temperature. This pair has not been detected by DLTS. However, Co_s does trap one or two H interstitials with binding energies 1.43 eV and 1.67 eV, respectively. Both complexes have an acceptor level in the gap, $\{Co_s,H\}$ at $E_c-0.27$ eV and $\{Co_s,H,H\}$ at $E_c-0.42$ eV. These DLTS lines are at $E_c-0.35$ eV and $E_c-0.29$ eV, respectively. They anneal out at and above 300 °C, respectively. These temperatures are consistent with the calculated binding energies.

Figure 5 shows that the acceptor levels move closer to the conduction band, as one goes from Co_s to $\{Co_s,H\}$ and then $\{Co_s,H,H\}$, a trend that suggests that adding more H can passivate Co_s. However, a complex such as $\{Co_s,H,H,H\}$ competes with $\{Co_s,H\}+H_2$ as well as with $Co_i + VH_3$: interstitial cobalt and a partially-saturated vacancy.[41]

Finally, the interactions between $^{3/2}Co_i^0$ and substitutional boron ($^0B_s^-$) lead to the formation of the $^{3/2}\{Co_i,B_s\}^-$ pair with a binding energy of 0.55 eV, slightly lower than the

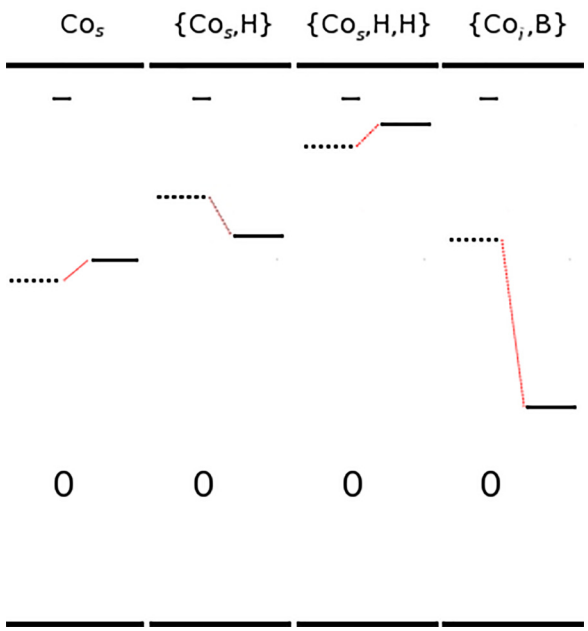

FIG. 5. Comparison of the calculated (dashed lines) and measured (solid lines[26]) gap levels associated with Co_s, $\{Co_s,H\}$, $\{Co_s,H,H\}$, and $\{Co_i,B_s\}$.

0.65 eV calculated for iron-boron at the same level of theory.[43] The $\{Co_iB_s\}$ pair is found to have an acceptor level at $E_c-0.36$ eV, unusually far from the measured $E_c-0.71$ eV.[26] We are unsure of the reason(s) for this discrepancy.

The comparison between the measured and calculated gap levels is shown in Fig. 5. No donor level has been associated with any Co-related defect in Si. The present calculations show no donor level either for any of the defects studied. This could be related to the $3d^9$ atomic configuration of Co that makes it more likely to trap an electron and become the closed-shell $3d^{10}$ negative ion than to trap a hole and become $3d^8$ positive ion.

ACKNOWLEDGMENTS

This work is supported in part by a grant from the Bay Area Photovoltaic Consortium. The Texas Advanced Computer Center and Texas Tech's High Performance Computer Center at Texas Tech provided generous amounts of computer time.

[1]A. A. Istratov and E. R. Weber, Appl. Phys. A **66**, 123 (1998).
[2]E. R. Weber, Appl. Phys. A **30**, 1 (1983).
[3]S. M. Myers, G. A. Petersen, and C. H. Seager, J. Appl. Phys. **80**, 3717 (1996).
[4]E. G. Moroni, R. Podloucky, and J. Hafner, Phys. Rev. Lett. **81**, 1969 (1998).
[5]J. R. Davis, Jr., A. Rohatgi, R. H. Hopkins, P. D. Blais, P. Rai-Choudhury, J. R. McCormick, and H. C. Mollenkopf, IEEE Trans. Electron Devices **ED-27**, 677 (1980); A. Rohatgi, J. R. Davis, R. H. Hopkins, P. Rai-Choudhury, P. G. Mcmullin, and J. R. McCormick, J. Solid State Electron. **23**, 415 (1980); A. Rohatgi and P. Rai-Choudhury, Sol. Cells **17**, 119 (1986).
[6]A. R. Peaker, V. P. Markevich, B. Hamilton, G. Parada, A. Dudas, A. Pap, E. Don, B. Lim, J. Schmidt, L. Yu, Y. Yoon, and G. Rozgonyi, Phys. Status Solidi A **209**, 1884 (2012).
[7]E. Scheibe and W. Schröter, Physica B **116**, 318 (1983).
[8]G. W. Ludwig and H. H. Woodbury, Solid State Phys. **13**, 223 (1962).
[9]D. J. Silva, U. Wahl, J. G. Correia, V. Augustyns, T. A. L. Lima, A. Costa, E. Bosne, M. R. da Silva, J. P. Araújo, and L. M. C. Pereira, Nucl. Instrum. Methods Phys. Res., Sect. B **371**, 59 (2016).
[10]H. Kitagawa and K. Hashimoto, Jpn. J. Appl. Phys., Part 1 **16**, 173–857 (1971).
[11]H. Nakashima and K. Hashimoto, Mater. Sci. Forum **83–87**, 227 (1992).
[12]J. Utzig and D. Gilles, Mater. Sci. Forum **38–41**, 729 (1989).
[13]W. Bergholz and W. Schröter, Phys. Status Solidi A **49**, 489 (1978).
[14]W. Bergholz, Physica B **116**, 312 (1983).
[15]H. Lemke, Phys. Status Solidi A **85**, K133 (1984).
[16]H. Kitagawa, H. Nakashima, and K. Hashimoto, Jpn. J. Appl. Phys., Part 1 **24**, 373 (1985).
[17]D. Mathiot, J. Appl. Phys. **65**, 1554 (1989).
[18]H. Nakashima, Y. Tsumori, T. Miyagawa, and K. Hashimoto, Jpn. J. Appl. Phys., Part 1 **29**, 1395 (1990).
[19]H. Nakashima, T. Sadoh, H. Kitagawa, and K. Hashimoto, Mater. Sci. Forum **143–147**, 761 (1994).
[20]K. Graff, *Metal Impurities in Silicon Device Fabrication* (Springer, Berlin, 1995).
[21]W. Jost, J. Weber, and H. Lemke, Semicond. Sci. Technol. **11**, 22 (1996).
[22]W. Jost, J. Weber, and H. Lemke, Semicond. Sci. Technol. **11**, 525 (1996).
[23]H. Kitagawa, Solid State Phenom. **71**, 51 (2000).
[24]H. Lemke and K. Irmscher, ECS Trans. **3**, 299 (2006).
[25]L. Scheffler, V. Kolkovsky, and J. Weber, Phys. Status Solidi A **209**, 1913 (2012).
[26]L. Scheffler, V. Kolkovsky, and J. Weber, J. Appl. Phys. **113**, 183714 (2013).
[27]J. Weber, L. Scheffler, V. Kolkovski, and N. Yarykin, Solid State Phenom. **205–206**, 245 (2014).
[28]L. A. Hemstreet, Phys. Rev. B **15**, 834 (1977).
[29]G. G. DeLeo, G. D. Watkins, and W. Beall Fowler, Phys. Rev. B **23**, 1851 (1981); **25**, 4962 (1982).
[30]A. Zunger and U. Lindefelt, Phys. Rev. **26**, 5989 (1982).
[31]H. Katayama-Yoshida and A. Zunger, Phys. Rev. B **31**, 8317 (1985).
[32]J. Utzig, J. Appl. Phys. **65**, 3868 (1989).
[33]F. Beeler, O. K. Anderson, and M. Scheffler, Phys. Rev. Lett. **55**, 1498 (1985).
[34]F. Beeler, O. K. Anderson, and M. Scheffler, Phys. Rev. B **41**, 1603 (1990).
[35]Y. Kamon, H. Harima, A. Yanase, and H. Katayama-Yoshida, Physica B **308–310**, 391 (2001).
[36]K. Matsukawa, K. Shirai, H. Yamaguchi, and H. Katayama-Yoshida, Physica B **401–402**, 151 (2007).
[37]Z. Z. Zhang, B. Partoens, K. Chang, and F. M. Peeters, Phys. Rev. B **77**, 155201 (2008).
[38]D. Sánchez-Portal, P. Ordejón, E. Artacho, and J. M. Soler, Int. J. Quant. Chem. **65**, 453 (1997).
[39]E. Artacho, D. Sánchez-Portal, P. Ordejón, A. García, and J. M. Soler, Phys. Status Solidi B **215**, 809 (1999).
[40]D. J. Backlund and S. K. Estreicher, Phys. Rev. B **81**, 235213 (2010).
[41]D. J. Backlund and S. K. Estreicher, Phys. Rev. B **82**, 155208 (2010).
[42]D. J. Backlund, T. M. Gibbons, and S. K. Estreicher, Phys. Rev. B **94**, 195210 (2016).
[43]M. Sanati, N. Gonzalez Szwacki, and S. K. Estreicher, Phys. Rev. B **76**, 125204 (2007).
[44]S. K. Estreicher, M. Sanati, and N. Gonzalez Szwacki, Phys. Rev. B **77**, 125214 (2008).
[45]N. Gonzalez Szwacki, M. Sanati, and S. K. Estreicher, Phys. Rev. B **78**, 113202 (2008).
[46]J. Lindroos, D. P. Fenning, D. Backlund, E. Verlage, A. Gorgulla, S. K. Estreicher, H. Savin, and T. Buonassisi, J. Appl. Phys. **113**, 204906 (2013).
[47]D. West, S. K. Estreicher, S. Knack, and J. Weber, Phys. Rev. B **68**, 035210 (2003).
[48]S. K. Estreicher, "Copper interaction with Silicon based materials: A survey," in *Materials Science in Semiconductor Processing*, edited by A. Mesli and O. Aboelfotoh (Elsevier, 2004), Vol. 7. No. 3, p. 101.
[49]A. Carvalho, D. J. Backlund, and S. K. Estreicher, Phys. Rev. B **84**, 155322 (2011).
[50]H. J. Monkhorst and J. D. Pack, Phys. Rev. B **13**, 5188 (1976).
[51]N. Troullier and J. L. Martins, Phys. Rev. B **43**, 1993 (1991).
[52]P. Rivero, V. M. García-Suárez, D. Pereñiguez, K. Utt, Y. Yang, L. Bellaiche, K. Park, J. Ferrer, and S. Barraza-Lopez, Comput. Mater. Sci. **98**, 372 (2015).

[53]B. Hammer, L. Hansen, and J. K. Nørskov, Phys. Rev. B **59**, 7413 (1999).
[54]S. K. Estreicher, D. J. Backlund, C. Carbogno, and M. Scheffler, Angew. Chem. **50**, 10221 (2011).
[55]O. F. Sankey and D. J. Niklevski, Phys. Rev. B **40**, 3979 (1989).
[56]O. F. Sankey, D. J. Niklevski, D. A. Drabold, and J. D. Dow, Phys. Rev. B **41**, 12750 (1990).
[57]A. Resende, R. Jones, S. Őberg, and P. R. Briddon, Phys. Rev. Lett. **82**, 2111 (1999).
[58]J. P. Goss, M. J. Shaw, and P. R. Briddon, in *Theory of Defects in Semiconductors*, edited by D. A. Drabold and S. K. Estreicher (Springer, Berlin, 2007), p. 69.
[59]G. Mills and H. Jonsson, Phys. Rev. Lett. **72**, 1124 (1994); H. Jonsson, G. Mills, and K. W. Jacobsen, in *Classical and Quantum Dynamics in Condensed Phase Simulations*, edited by B. J. Berne, G. Ciccotti, and D. F. Coker (World Scientific, Singapore, 1998), p. 385.
[60]G. Henkelman, B. P. Uberuaga, and H. Jonsson, J. Chem. Phys. **113**, 9901 (2000).
[61]G. Henkelman and H. Jonsson, J. Chem. Phys. **113**, 9978 (2000).
[62]A. A. Istratov, C. Flink, H. Hieslmair, E. R. Weber, and T. Heiser, Phys. Rev. Lett. **81**, 1243 (1998).
[63]G. D. Watkins, in *Deep Centers in Semiconductors*, edited by S. T. Pantelides (Gordon and Breach, New York, 1986), p. 147.
[64]G. D. Watkins and J. R. Troxell, Phys. Rev. Lett. **44**, 593 (1980).
[65]S. Dannefaer, P. Mascher, and D. Kerr, Phys. Rev. Lett. **56**, 2195 (1986).
[66]R. Kube, H. Bracht, E. Hűger, H. Schmidt, J. Lundsgaard Hansen, A. Nylandsted Larsen, J. W. Ager III, E. E. Haller, T. Geue, and J. Stahn, Phys. Rev. B **88**, 085206 (2013).
[67]T. Sudkamp and H. Bracht, Phys. Rev. B **94**, 125208 (2016).
[68]S. K. Estreicher, Phys. Status Solidi B **217**, 513 (2000).
[69]S. K. Estreicher, M. Sanati, D. West, and F. Ruymgaart, Phys. Rev. B **70**, 125209 (2004).
[70]D. E. Woon, D. S. Marynick, and S. K. Estreicher, Phys. Rev. B **45**, 13383 (1992).
[71]R. H. Hall and J. H. Racette, J. Appl. Phys. **35**, 379 (1964).
[72]M. K. Bakhadyrkhanov, S. Zainabidinov, and A. Khamidov, Sov. Phys. Semicond. **14**, 243 (1980).